

Numerical Analysis of Viscous Vortex Motion

by

U MYA OO (ウー ミヤ ウー)

Department of Applied Science, Faculty of Engineering,
Kyushu University, Hakozaki, Fukuoka 812

Head-on collision of two co-axial viscous vortex rings is simulated by numerical integration of the Navier-Stokes equations for viscous incompressible fluid. Numerical results are employed to observe the behaviors of the time dependent flow quantities and confirm the importance of viscosity. Sudden decrease of the total energy and circulation subsequent to the period of their conservation, is observed to be similar to the phenomenon of the energy catastrophe studied in the turbulence theory.

1. Introduction

Recent experimental and theoretical investigation^{1,2)} upon acoustic wave generated by head-on collision of two vortex rings has stressed importance of viscosity as a dominant factor in determining the form of the acoustic signal emitted by the vortex motion. The results of their work also indicate the need to study the viscous motion of high Reynolds number.

In the inviscid fluid the head-on collision of two co-axial vortex rings possessing the same strength and the same size is

considered to be equivalent to the motion of one ring approaching a plane perpendicular to its axis. In this case the image inside the wall acts as the other ring.

However because of the symmetry of the vortex configuration, similar application can be made to the motion of viscous fluid. The principal difference from the inviscid case is that the total kinetic energy and the vortex strength are no longer conserved during the motion, due to the viscous diffusion of vorticity.

Thus the aim of the present study is to determine the behavior of time dependent flow quantities at high Reynolds numbers, by applying the Navier-Stokes equation to the motion of a viscous incompressible fluid. The Navier-Stokes equation and the continuity equation are transformed into the equations of vorticity and stream function. They are then solved by means of finite difference approximations for appropriate boundary conditions and given initial vorticity distributions. The numerical method used here is expected to give accurate results only for low and medium Reynolds numbers. However it is hoped that through these analyses one can get an idea about the behavior of viscous vortex motion at higher Reynolds numbers.

Recently collision of a single vortex ring with a solid wall was investigated experimentally by Yamada et al.³⁾, finding generation of a secondary vortex ring at the wall in addition to the main vortex. In comparison with the present study where stress-free condition is applied at the plane boundary, viscosity effect is enhanced in their experiment by the presence of the rigid wall where no-slip condition is imposed.

2. Mathematical formulation

2.1 Governing equations

We consider an axisymmetric flow without swirl of an incompressible viscous flow in cylindrical polar co-ordinates (x, r, ϕ) with the axis x coincident with the symmetry axis of the vortex. In view of the property that all the flow quantities are independent of the azimuthal angle ϕ , we have the velocity components $(u(x, r), v(x, r), 0)$ and the vorticity $(0, 0, \omega(x, r))$. The governing equations of the unsteady incompressible viscous flow are the Navier-Stokes equation for the vorticity and the continuity equation :

$$\frac{\partial \omega}{\partial t} + u \frac{\partial \omega}{\partial x} + v \frac{\partial \omega}{\partial r} = \nu \left(\frac{\partial^2 \omega}{\partial x^2} + \frac{\partial^2 \omega}{\partial r^2} + \frac{1}{r} \frac{\partial \omega}{\partial r} - \frac{\omega}{r^2} \right), \quad (2.1)$$

$$\frac{\partial u}{\partial x} + \frac{\partial v}{\partial r} = 0, \quad (2.2)$$

together with the relations

$$u = \frac{1}{r} \frac{\partial \psi}{\partial r}, \quad v = -\frac{1}{r} \frac{\partial \psi}{\partial x}, \quad (2.3)$$

$$\omega = \frac{\partial v}{\partial x} - \frac{\partial u}{\partial r}, \quad (2.4)$$

where ψ is the Stokes stream function, ν the kinematic viscosity and t the time.

To obtain the equivalent system of equations to be approximated by the finite difference equations, we transform the above eq.(2.1), using eq.(2.2), into the following conservation form:

$$\frac{\partial \omega}{\partial t} + \frac{\partial u \omega}{\partial x} + \frac{\partial v \omega}{\partial r} = \nu \left(\frac{\partial^2 \omega}{\partial x^2} + \frac{\partial^2 \omega}{\partial r^2} + \frac{1}{r} \frac{\partial \omega}{\partial r} - \frac{\omega}{r^2} \right), \quad (2.5)$$

in anticipation of the fact that the equation of motion in the

form of conservation law is more effective for convergence of the numerical iterations.

Using the eq.(2.3), the expression (2.4) can be transformed into the relation

$$\frac{\partial^2 \psi}{\partial x^2} + \frac{\partial^2 \psi}{\partial \sigma^2} - \frac{1}{\sigma} \frac{\partial \psi}{\partial \sigma} = -\sigma \omega \quad (2.6)$$

Let us take the radius a of the vortex ring at an initial position as the reference length and a magnitude of vorticity in the vortex core as the reference vorticity and define

$$x = a x^* \quad , \quad \sigma = a \sigma^* \quad , \quad \omega = \Omega_0 \omega^* \quad , \quad u = a \Omega_0 u^* \quad , \quad v = a \Omega_0 v^* \quad , \\ t = \Omega_0^{-1} t^* \quad , \quad \psi = a^3 \Omega_0 \psi^* \quad .$$

With these substitutions, eqs. (2.3), (2.5) and (2.6) retain the same form (for convenience the asterisk can be dropped) except all quantities are dimensionless and ν is replaced by $1/Re$, where Re is the Reynolds number defined as $Re = a^2 \Omega_0 / \nu$.

2.2 Initial and boundary conditions

The plane wall against which the vortex collides is taken at $x = 0$. In view of the axisymmetric nature of the problem, we consider the vortex motion in the region $(0 < x < \infty, 0 \leq \sigma < \infty)$.

The initial state of the vortex ring is assumed to have a compact vortex core, that is, the vorticity at $t = 0$ takes a non-zero value C (with dimensional value $C \Omega_0$) only in a compact domain D of the $x-\sigma$ plane :

$$\omega \Big|_{t=0} = \begin{array}{ll} C , & \text{inside } D, \\ 0 , & \text{outside } D. \end{array} \quad (2.7)$$

A circular form is assumed for D: $\{(x, \sigma) / [(x - X_c)^2 + (\sigma - 1)^2]^{1/2} \leq 0.3\}$, where $X_c (> 0)$ is the initial mean axial position of the vortex and the core radius is taken as 0.3. The initial value of vorticity $C = -2.0$ is used throughout D, where the minus sign means that the vortex motion is to the wall at $x = 0$.

In order to improve the final results obtained from the computation, we employed another initial condition derived from the above condition, in which D is not necessarily circular and C is not constant.

The boundary condition on the symmetry axis $\sigma = 0$ is that $v = 0$ and $\partial u / \partial \sigma = 0$ hold by the symmetry of the velocity field. The conditions at the wall are $u = 0$ and $\partial v / \partial x = 0$. Those conditions are transformed into the conditions

$$\psi = 0 \text{ and } \omega = 0 \text{ on } \sigma = 0 \text{ and } x = 0, \quad (2.8)$$

which manifest that the boundaries $\sigma = 0$ and $x = 0$ are coincident with a streamline and viscous stress vanishes there.

For the conditions at infinity we take

$$\omega = 0 \text{ and } \psi = 0, \quad (2.9)$$

since the velocity field induced by vortex rings is irrotational and decays as $O(r^{-3})$ where $r = \sqrt{x^2 + \sigma^2}$.

2.3 The analytical expressions

For later use, it is desirable to get definitions of some flow quantities as follows.

The circulation of the system can be defined as

$$\Gamma = \iint_A \omega dx d\sigma, \quad (2.10)$$

where A denote the domain considered on the axial plane (x, σ) . The coordinates of the center of vortex core can be defined by the expressions ;

$$\bar{x} = \frac{\iint_A \omega x dx d\sigma}{\Gamma}, \quad \bar{\sigma} = \frac{\iint_A \omega \sigma dx d\sigma}{\Gamma}. \quad (2.11)$$

The total kinetic energy E of the system and its time derivatives can be expressed as follows ;

$$\begin{aligned} E &= \frac{1}{2} \iint_A \{ u^2 + v^2 \} 2\pi \sigma dx d\sigma \\ &= \pi \iint_A \omega \varphi dx d\sigma, \end{aligned} \quad (2.12)$$

$$\frac{dE}{dt} = -\frac{2\pi}{Re} \iint_A \omega^2 \sigma dx d\sigma, \quad (2.13)$$

$$\frac{d^2 E}{dt^2} = -\frac{2}{Re} \iint_A \omega^2 \sigma dx d\sigma + \frac{2}{Re^2} \iint_A \left\{ \left(\frac{\partial \omega}{\partial x} \right)^2 + \left(\frac{\partial \omega}{\partial \sigma} \right)^2 + \left(\frac{\omega}{\sigma} \right)^2 \right\} \sigma dx d\sigma. \quad (2.14)$$

3. Finite difference equations

To solve the time dependent problem corresponding to the required physical situation, we use the finite difference equations approximating the eqs. (2.3), (2.5) and (2.6) (in dimensionless form) . To construct the finite difference equations we divide the region of consideration in the $x-\sigma$ plane into rectangular meshes whoses intervals are taken as h and k in the x and σ directions respectively. The numbers of the mesh points in the corresponding directions are denoted by I and J respectively. The network of mesh points is shown in Fig.1. Here we consider the finite region OABC with such an extent that the boundary condition (2.9) at infinity is replaced with the suffi-

cient accuracy by $\psi = 0$ and $\omega = 0$ on the two sides AB and BC in Fig.1 . Therefore the two conditions (2.8) and (2.9) reduce to the boundary conditions :

$$\psi = 0 \quad \text{and} \quad \omega = 0 \quad \text{on all the boundaries OA, AB, BC and CO ,} \quad (3.1)$$

for the computation of the finite difference equations.

Time step is taken as τ and the values of ψ , ω , u and v at the point (ih, jk) and at the time $t = n\tau$ are denoted by ψ_{ij}^n , ω_{ij}^n , u_{ij}^n and v_{ij}^n respectively, where i and j are integers.

Using the above notations and substituting the forward difference formula for time derivative and the central difference formulae for space derivatives into the eqs. (2.5) and (2.6), we obtain the following finite difference equations:

$$\begin{aligned} \frac{\omega_{ij}^{n+1} - \omega_{ij}^n}{\tau} &= - \left\{ \frac{(u\omega)_{i+1,j}^n - (u\omega)_{i-1,j}^n}{2h} + \frac{(v\omega)_{i,j+1}^n - (v\omega)_{i,j-1}^n}{2k} \right\} + \frac{1}{Re} \left\{ \frac{\omega_{i+1,j}^n + \omega_{i-1,j}^n - 2\omega_{ij}^n}{h^2} \right. \\ &\quad \left. + \frac{\omega_{i,j+1}^n + \omega_{i,j-1}^n - 2\omega_{ij}^n}{k^2} + \frac{1}{\sigma} \frac{\omega_{i,j+1}^n - \omega_{i,j-1}^n}{2k} - \frac{\omega_{i,j}^n}{\sigma^2} \right\} \\ &= \mathcal{L}_\tau^m(\omega) + \mathcal{L}_x^m(\omega) \quad , \quad (3.2) \end{aligned}$$

$$\mathcal{L}_x^s(\omega) = - \left\{ \frac{(u\omega)_{i+1,j}^s - (u\omega)_{i-1,j}^s}{2h} \right\} + \frac{1}{Re} \left\{ \frac{\omega_{i+1,j}^s + \omega_{i-1,j}^s - 2\omega_{ij}^s}{h^2} \right\} \quad , \quad (3.3)$$

$$\begin{aligned} \mathcal{L}_\tau^s(\omega) &= - \left\{ \frac{(v\omega)_{i,j+1}^s - (v\omega)_{i,j-1}^s}{2k} \right\} + \frac{1}{Re} \left\{ \frac{\omega_{i,j+1}^s + \omega_{i,j-1}^s - 2\omega_{ij}^s}{k^2} + \right. \\ &\quad \left. \frac{1}{\sigma} \frac{\omega_{i,j+1}^s - \omega_{i,j-1}^s}{2k} - \frac{\omega_{i,j}^s}{\sigma^2} \right\} \quad , \quad (3.4) \end{aligned}$$

$$s = n \quad ,$$

$$\frac{\psi_{i-1,j}^n + \psi_{i+1,j}^n - 2\psi_{i,j}^n}{h^2} + \frac{\psi_{i,j-1}^n + \psi_{i,j+1}^n - 2\psi_{i,j}^n}{k^2} - \frac{1}{\sigma} \frac{\psi_{i,j+1}^n - \psi_{i,j-1}^n}{2k} = -\sigma \omega_{i,j}^n \quad (3.5)$$

For eq.(2.3) finite difference approximations can be made as follows. Let us denote the values of a function $f(x)$ and its derivatives at $x = ih$ by t_i, t_i', t_i'' and so on. Then, using Taylor series expansions of $t_{i-1}, t_{i+1}, t_{i-1}'$ and t_{i+1}' , we can write

$$t_{i-1}' + 4t_i' + t_{i+1}' = \frac{3}{h} (t_{i+1} - t_{i-1}) + O(h^4),$$

which is in tridiagonal form and gives the first derivatives of t_i in terms of t_i to the accuracy of fourth order of h .

Employing the above formula to the calculation of the velocity components $u_{i,j}$ and $v_{i,j}$ from eq.(2.3), we obtain the finite difference equations

$$(\sigma u)_{i,j-1} + 4(\sigma u)_{i,j} + (\sigma u)_{i,j+1} = \frac{3}{k} (\psi_{i,j+1} - \psi_{i,j-1}), \quad (3.6)$$

$$(\sigma v)_{i-1,j} + 4(\sigma v)_{i,j} + (\sigma v)_{i+1,j} = -\frac{3}{h} (\psi_{i+1,j} - \psi_{i-1,j}). \quad (3.7)$$

To solve the difference equation (3.2), we apply the method based on that devised by Peaceman & Rachford⁴⁾ for diffusion problems, known as ADI (Alternating Direction Implicit) method. Thus each time step, $n\tau$ to $(n+1)\tau$, is divided into two successive half steps, $n\tau$ to $(n+1/2)\tau$ and $(n+1/2)\tau$ to $(n+1)\tau$, and hence eq.(3.2) becomes

$$\frac{\omega_{i,j}^{n+1/2} - \omega_{i,j}^n}{\tau/2} = \mathcal{L}_\sigma(\omega) + \mathcal{L}_x(\omega), \quad (3.8)$$

$$\frac{\omega_{i,j}^{n+1} - \omega_{i,j}^{n+\frac{1}{2}}}{\tau/2} = \mathcal{L}_y^{n+1}(\omega) + \mathcal{L}_x^{n+\frac{1}{2}}(\omega), \quad (3.9)$$

where $\mathcal{L}_y^m(\omega)$, $\mathcal{L}_y^{n+1}(\omega)$ and $\mathcal{L}_x^{n+\frac{1}{2}}(\omega)$ are as defined in eqs. (3.3) and (3.4).

Since eqs. (3.6)-(3.9) are the systems of equations in tridiagonal forms, we can apply Gauss elimination method to solve eqs. (3.6) and (3.7) for $u_{i,j}$ and $v_{i,j}$ from known values of $\psi_{i,j}$, eq. (3.8) for $\omega_{i,j}^{n+\frac{1}{2}}$ and eq. (3.9) for $\omega_{i,j}^{n+1}$.

To solve eq. (3.5), we use SOR (Successive Over-Relaxation) method after modifying the equation as

$$\psi_{i,j}^{s+1} = (1-\alpha)\psi_{i,j}^s + \frac{\alpha}{2(h^2+k^2)} \left\{ \frac{\psi_{i+1,j}^s + \psi_{i-1,j}^{s+1}}{h^2} + \frac{\psi_{i,j+1}^s + \psi_{i,j-1}^{s+1}}{k^2} - \frac{1}{\sigma} \frac{\psi_{i,j+1}^s - \psi_{i,j-1}^{s+1}}{2k} + \sigma \omega_{i,j}^m \right\}, \quad (3.10)$$

where α is the parameter known as the relaxation factor and the index s indicates the number of the iteration times. In this formula the latest possible values of $\psi_{i,j}$ are substituted in the right hand side for the rapid rate of convergence of the iterations and the optimum value of α has been chosen based on the formulae $\alpha = \frac{8-4\sqrt{4-\beta^2}}{\beta^2}$ and $\beta = \cos \frac{\pi}{I} + \cos \frac{\pi}{J}$ 5) and some trial test. Here I and J are the numbers of mesh points as stated above.

4. Computational procedure

4.1 Initial condition

Initially all dependent variables were set to zero except

the vorticity for which we assigned $\omega_{ij} = -2$ for the points which lie in the core $\{(x, \sigma) : ((x - X_c)^2 + (\sigma - 1)^2)^{1/2} \leq 0.3\}$ and $\omega_{ij} = 0$ for the remaining points. Here $(X_c, 1)$ and 0.3 are the initial coordinates of the core center and the core radius respectively.

Next, using the assigned values of ω_{ij} and ψ_{ij} we improved the values of ψ_{ij} by eq. (3.10). The iteration was continued until the two successive values of ψ_{ij}^k and ψ_{ij}^{k+1} had met the convergence condition $|\psi_{ij}^{k+1} - \psi_{ij}^k| < 10^{-6}$ (at $k = K$). Taking the given values of ω_{ij} and the converged values of ψ_{ij} as the initial values we proceeded to the next time $t = \tau, 2\tau, 3\tau, \dots$. The procedure from the time $t = n\tau$ to the next time $t = (n+1)\tau$ is described in the next sub-section 4.2.

Up to here we have assumed that the initial shape of vortex core is exactly circle and approximated the initial vorticity distribution by giving uniform values for mesh points which lie in the circle and zero for outside points. However the actual shape of the vortex core may be not necessarily circle and vorticity distribution in the core may not be exactly uniform. For this reason we devised the way to get the better approximation of the initial shape of vortex core and the vorticity distribution in it. We recorded the vorticity distribution at an appropriate time after proceeding the above computation with the previous initial conditions, and the equi-vorticity lines for that time were plotted.

From this procedure we obtained the more suitable set of vorticity distribution which would give a reasonable shape of vortex core and the vorticity distribution in the core region

in the state of translational motion. Thus we assigned the new initial vorticity distribution by constructing the vortex core which has the same shape and the same vorticity distribution in it as those of the core of vortex given by the recorded data. The size of the core was also chosen by specifying a minimum value of the vorticity below which the value of ω_{ij} was set equal to zero. The center of the core was made to coincide with the position of the previous initial core center. The other dependent variables are all set to zero for all points as in the previous initial conditions. From those values, the values of ψ_{ij} were modified by the eq.(3.10) and the same procedure continued as stated previously.

4.2 The steps required to proceed from time $n\tau$ to time $(n+1)\tau$

Let us suppose that the values of ω_{ij}^n , ψ_{ij}^n , u_{ij}^n and σ_{ij}^n are known up to the time $n\tau$, where those of u_{ij}^n and σ_{ij}^n are determined from the relations (3.6) and (3.7), then the values of ω_{ij}^{n+1} , ψ_{ij}^{n+1} , u_{ij}^{n+1} and σ_{ij}^{n+1} for the next time $(n+1)\tau$ can be calculated as follows.

1. Using the formula $\psi_{ij}^{n+1} = \psi_{ij}^n + (\psi_{ij}^n - \psi_{ij}^{n-1})$, we approximate the values of ψ_{ij}^{n+1} .
2. Then the values of u_{ij}^{n+1} and σ_{ij}^{n+1} can be calculated by using eqs.(3.6) and (3.7).
3. Systems of equations, eqs.(3.8) and (3.9), are solved to get ω_{ij}^{n+1} and ω_{ij}^{n+1} by using ADI method.
4. Next, using the up-to-date values of ω_{ij}^{n+1} we solve eq.(3.10) to get the corrected values of ψ_{ij}^{n+1} by SOR method. The iteration

was continued until the two successive values of ψ_{ij}^s and ψ_{ij}^{s+1} satisfy the condition $\left| \frac{\psi_{ij}^{s+1} - \psi_{ij}^s}{\psi_{ij}^s} \right| < 10^{-5}$ where ψ_{ij}^s denotes the reference value of ψ_{ij} , taken as the maximum value of ψ_{ij} at $t=0$ in this case.

5. Using the latest revised values of ψ_{ij}^{n+1} we repeat step 2 to step 4 again and again until the values of ω_{ij}^{n+1} no longer change. The convergency of the whole iteration process was tested by the condition $\left| (\omega_{ij}^{n+1})^{k+1} - (\omega_{ij}^{n+1})^k \right| < 10^{-5}$ where k and $k+1$ denote the numbers of the successive iterations.

6. When the convergence condition in the step 5 is satisfied the latest values of ω_{ij}^{n+1} and ψ_{ij}^{n+1} together with u_{ij}^{n+1} and v_{ij}^{n+1} are taken as the values for the time $(n+1)\tau$. Thus one time step is completed and we can proceed to the next time step in the same way.

5. Results and discussion

Computations were carried out by taking the grid points of 136×121 and the size of the space step $1/15$ for both x and y directions. It was found that a further increment in the size of the region did not produce any noticeable changes of the results. It therefore confirms the chosen size of the region is sufficiently large to approximate the infinite region of the required flow field.

The error bounds for the values of ψ_{ij} and ω_{ij} are that a further reduction of them brought no improvement of the accuracy of the solutions, at least for four significant figures. The accuracy of the procedure is also checked by using the analytical

expressions (2.12)-(2.14) for E , dE/dt , d^2E/dt^2 as shown in Table(1).

Figures 2(a) to 2(d) show the equi-vorticity lines and streamlines at $t = 0, 39.8, 49.8$ and 59.8 for $Re = 500, 1000, 2500$ and 5000 . Figure 3 shows the paths of the centroid of vorticity defined in eq.(2.11), where the ordinate gives the radius of the vortex ring at the corresponding position. It can be seen from the figure that the radius of the vortex remains almost constant till the vortex reaches at a distance of the order of its core radius from the wall and after that it increases rapidly.

Figure 4 represents the variation of the circulation defined in eq.(2.10), and fig,5 the variation of energy of the system defined by eq.(2.12), both plotted against the dimensionless time t^* for $Re = 500, 2500$ and 5000 . Comparing with the curves of the vortex path, it is found that as the Reynolds number increases from 500, to 5000, the energy and the circulation curves tend to be flat for the vortex positions away from the wall, and decrease after the vortex has reached very near to the wall. This indicates that the effect of viscosity becomes dominant as the vortex comes close to the wall at distances of the order radius of the core. It appears that, as the Reynolds number is increased indefinitely, the circulation and the energy of the system tend to be conserved in an initial period and then suddenly damped by the viscous action when the vortex comes near the wall. This sort of behavior of total energy, that is, initial conservation and subsequent sudden increase, is called as energy catastrophe in the theory of homogeneous turbulence by Andre and Lesieur⁶⁾.

In Fig.6 , the distribution of vorticity across the diameter parallel to the symmetry axis is plotted for $t = 49.8$ and 59.8 for $Re = 2500$.. From the figure it can be seen that the vorticity distributions compare fairly well with the Gaussian distribution. Figure 7 shows the variations of maximum vorticity with time t and it can be seen that near $t = 50$ the maximum vorticity increases abruptly and subsequently decreases. This increase is probably due to the stretching of vortex when it collides against the wall, and the subsequent decrease is due to viscous dissipation. Considering the fact that this case of a single vortex colliding against the wall is equivalent to that of head-on collision of two vortices, the viscous decay of the total circulation of the single vortex implies pair annihilation of positive and negative vorticities.

6. Conclusion

Although the Reynolds numbers used in the present study were not strictly comparable to that of ref.1 and 2), it can be said that our results confirm the important role played by viscosity when the cores of two vortex rings come into collision. Therefore this analysis suggests that the acoustic emission studied in ref.2) must have been affected largely by the action of viscosity.

It is interesting to note that the viscous decay of the total circulation of the single vortex is interpreted as pair annihilation of the vorticities of opposite senses, and that the sudden decrease of the energy and circulation is subsequent to the period of their conservation is observed to be similar to the phenomenon of the energy catastrophe studied in the turbulence theory.

References

- 1) T.Minota and T.Kambe : 九大工学集報 ,55 (昭和 57年),pp 1.
- 2) T.Kambe and T.Minota : Submitted to Proc.Roy.Soc(London).
- 3) H.Yamada, T.Kohsaka, H.Yamabe and T.Matsui : J.Phys.Soc.Jpn.
51 (1982) 1663 .
- 4) D.W.Peaceman and H.H.Rachford : J.Soc.Indust.Applied Math.
3 (1955) 28 .
- 5) C.Y.Chow : An Introduction to Computational Fluid Mechanics,
(John Wiley & Sons,1979) Chap.2 .
- 6) J.C.Andre and M.Lesieur : J.Fluid Mech.(1977), vol.81,
part 1, 187-207 .

t \ Re		500	1000	2500	5000
10.	NE	-1.074×10^{-3}	-8.875×10^{-4}	-5.420×10^{-4}	-2.670×10^{-4}
	AE	-1.074×10^{-3}	-8.875×10^{-4}	-5.388×10^{-4}	-2.689×10^{-4}
30.	NE	-5.490×10^{-4}	-5.335×10^{-4}	-3.950×10^{-4}	-2.235×10^{-4}
	AE	-5.481×10^{-4}	-5.323×10^{-4}	-3.928×10^{-4}	-2.221×10^{-4}
50.	NE	-3.555×10^{-4}	-4.305×10^{-4}	-5.410×10^{-4}	-3.265×10^{-4}
	AE	-3.555×10^{-4}	-4.220×10^{-4}	-4.870×10^{-4}	-2.671×10^{-4}
10.	NEE	4.635×10^{-5}	2.790×10^{-5}	1.040×10^{-5}	4.208×10^{-6}
	AEE	4.480×10^{-5}	2.646×10^{-5}	0.942×10^{-5}	3.979×10^{-6}
30.	NEE	1.465×10^{-5}	1.093×10^{-5}	4.908×10^{-6}	2.043×10^{-6}
	AEE	1.423×10^{-5}	1.038×10^{-5}	4.526×10^{-6}	1.875×10^{-6}
50.	NEE	5.208×10^{-6}	-4.370×10^{-6}	-3.980×10^{-5}	-1.952×10^{-5}
	AEE	5.017×10^{-6}	-4.652×10^{-6}	-4.077×10^{-5}	-2.004×10^{-5}

NE =Numerically obtained value of dE/dt

AE =Analytically obtained value of dE/dt

NEE =Numerically obtained value of d^2E/dt^2

AEE =Analytically obtained value of d^2E/dt^2

Table 1 .

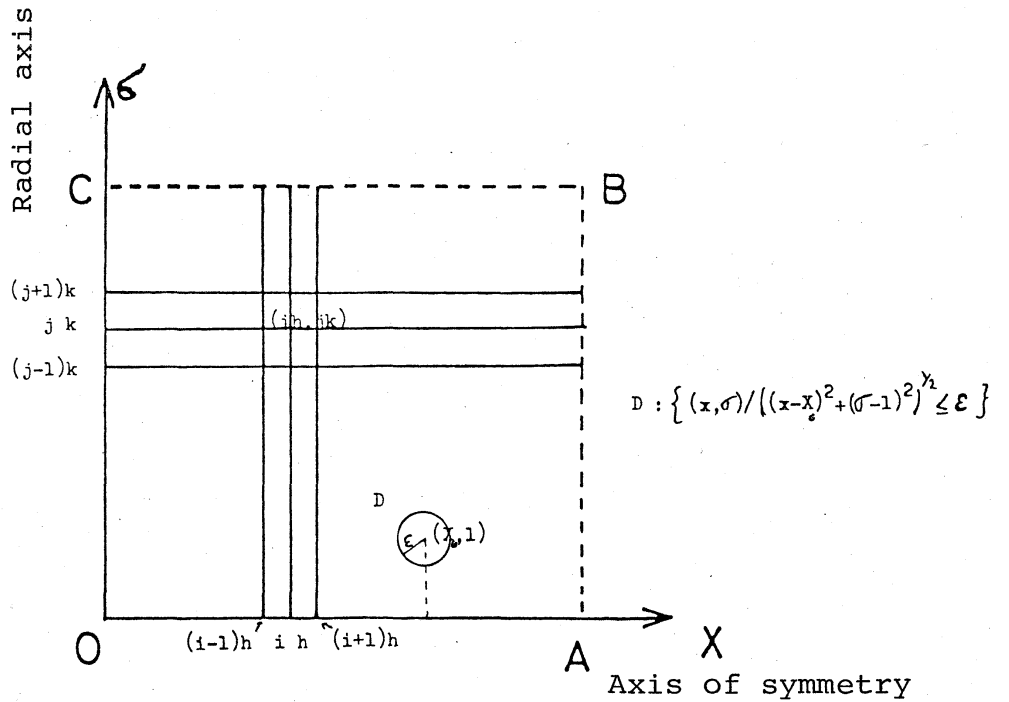
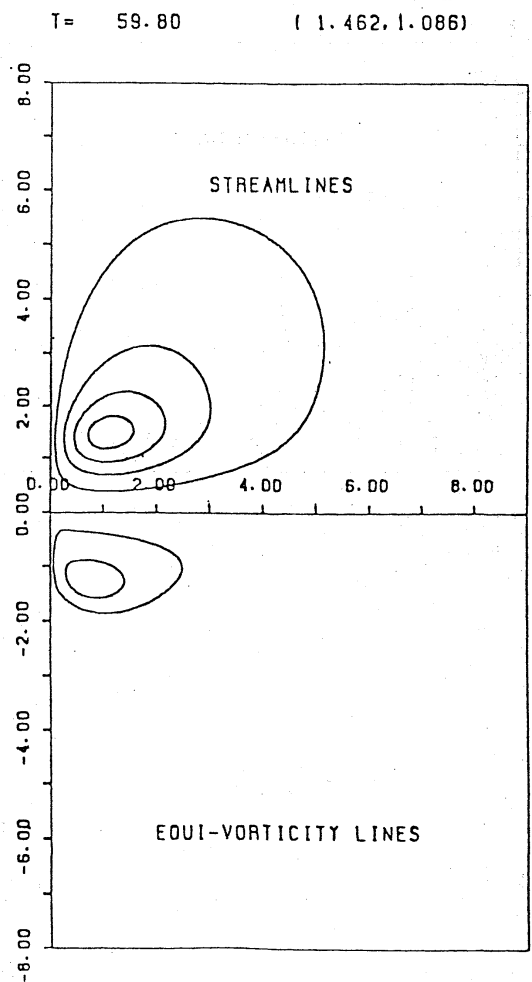
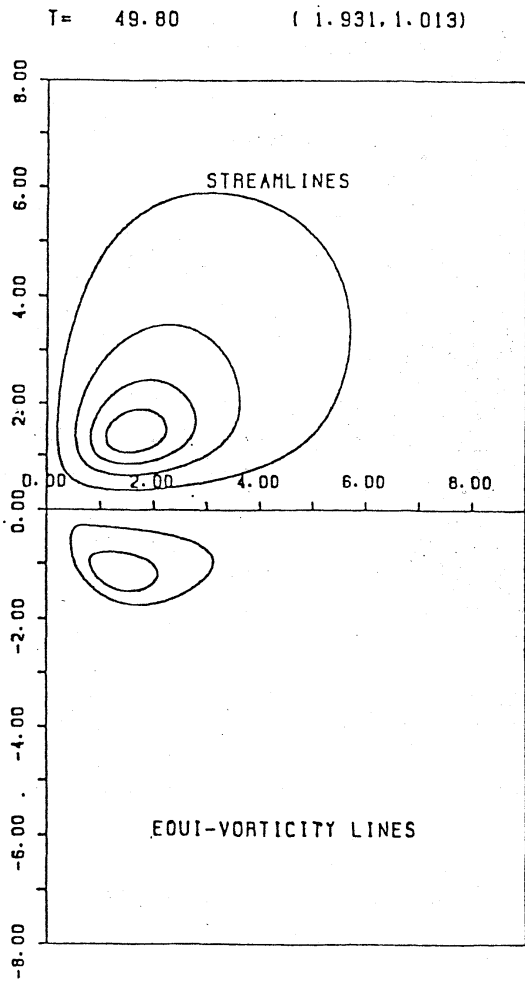
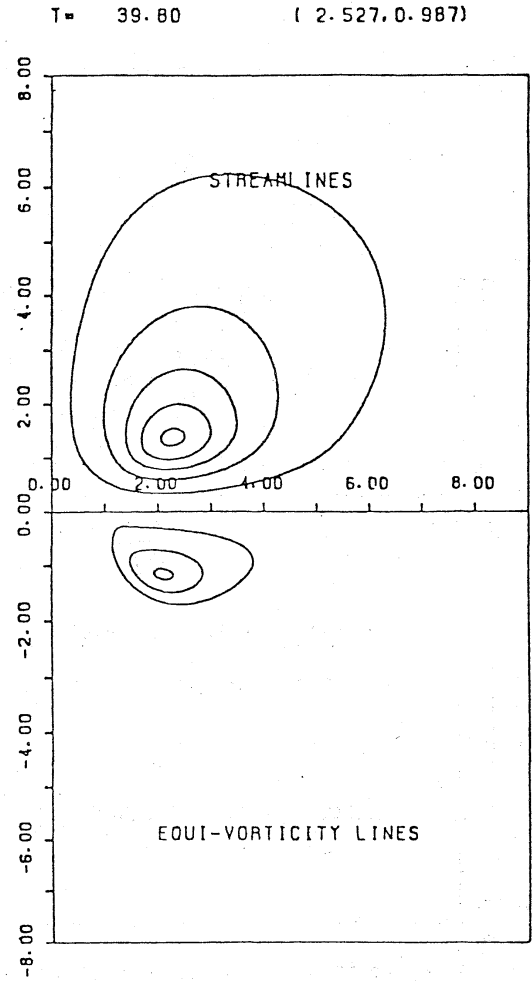
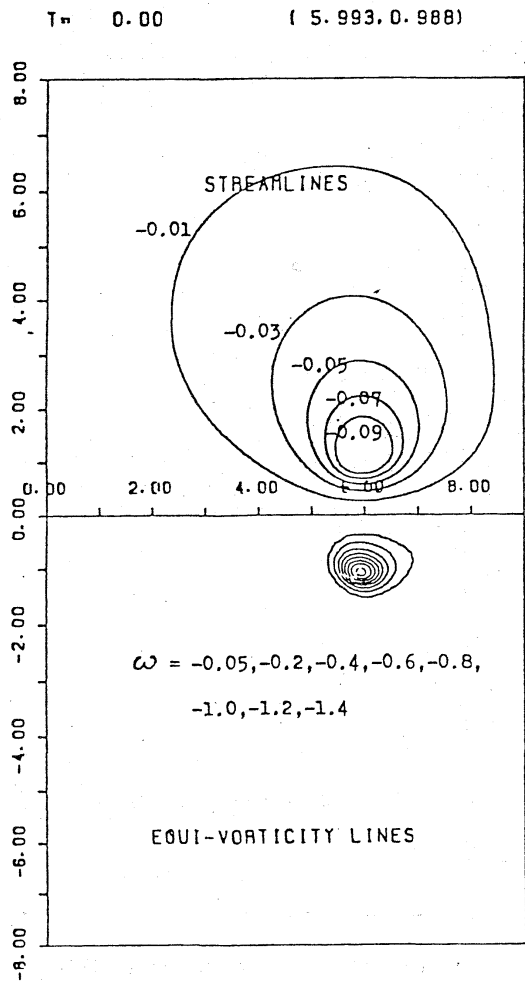
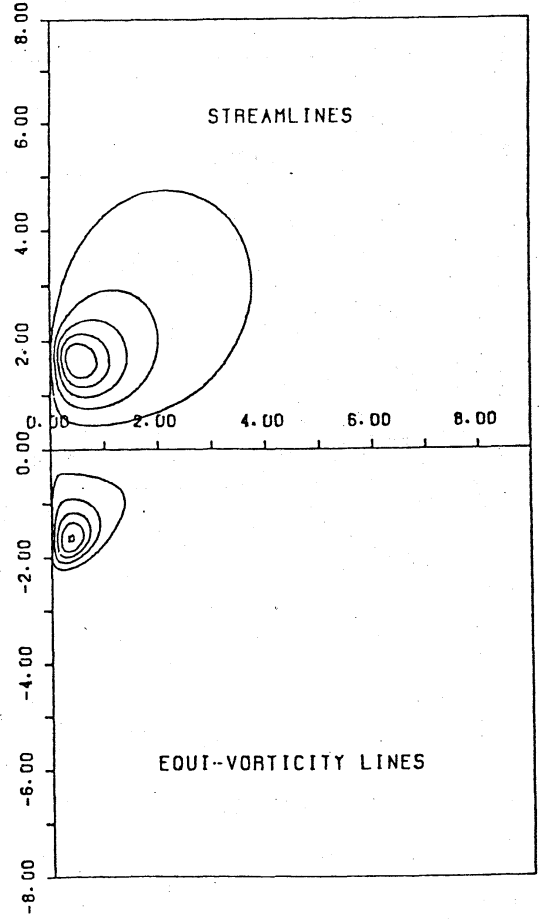
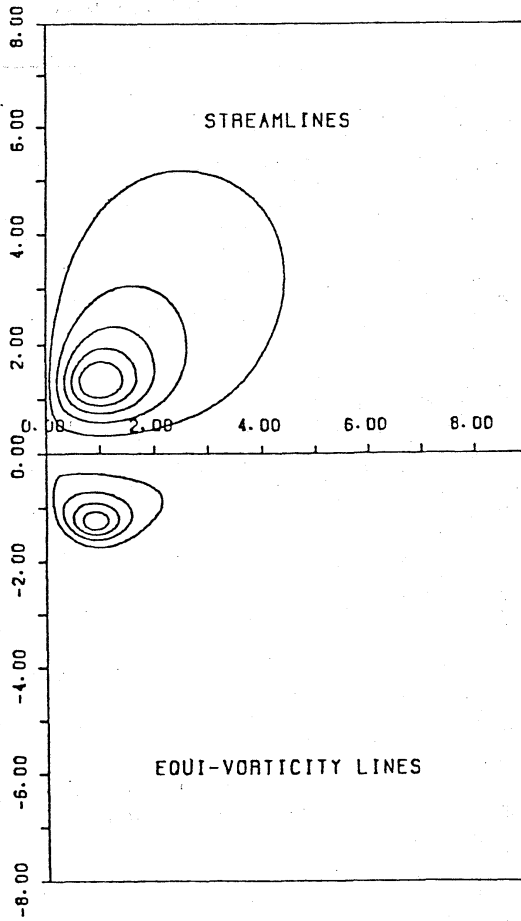
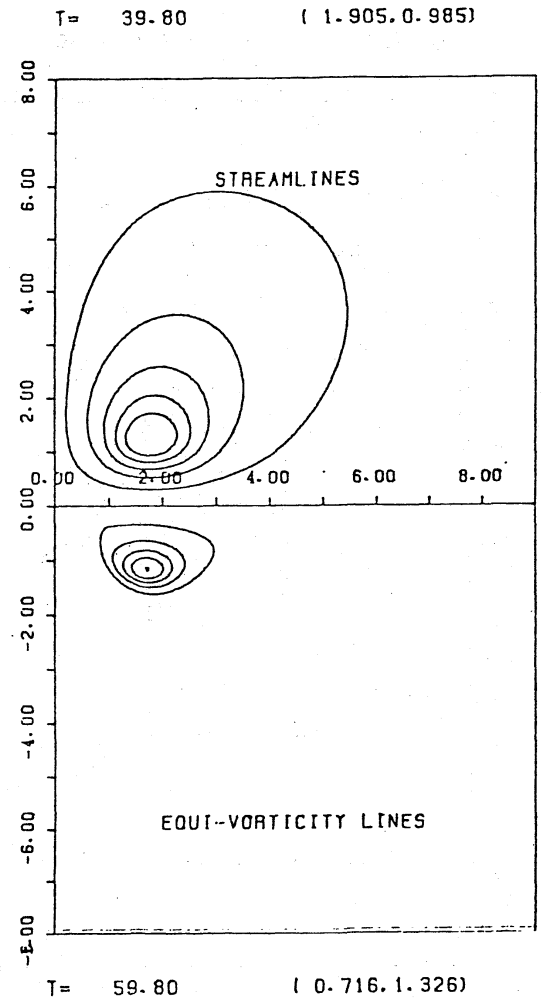
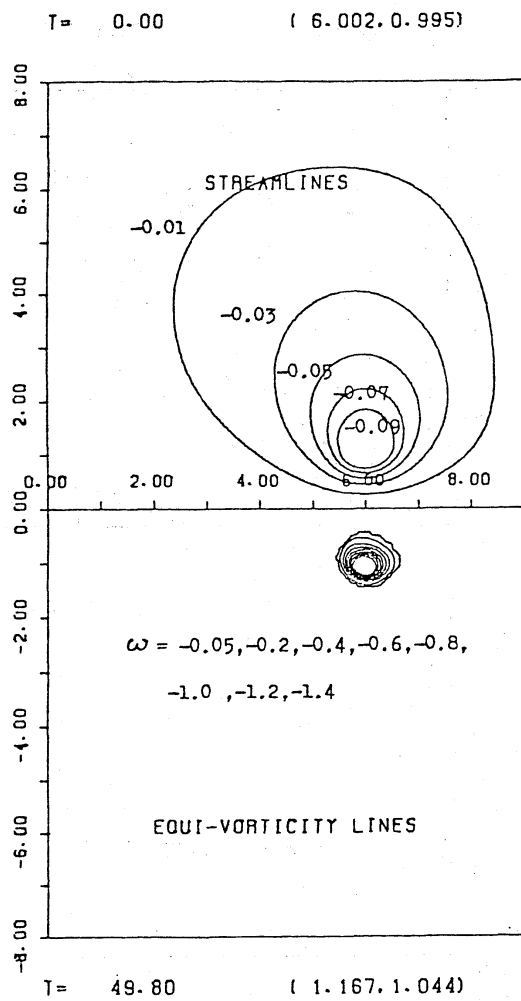


Fig.1

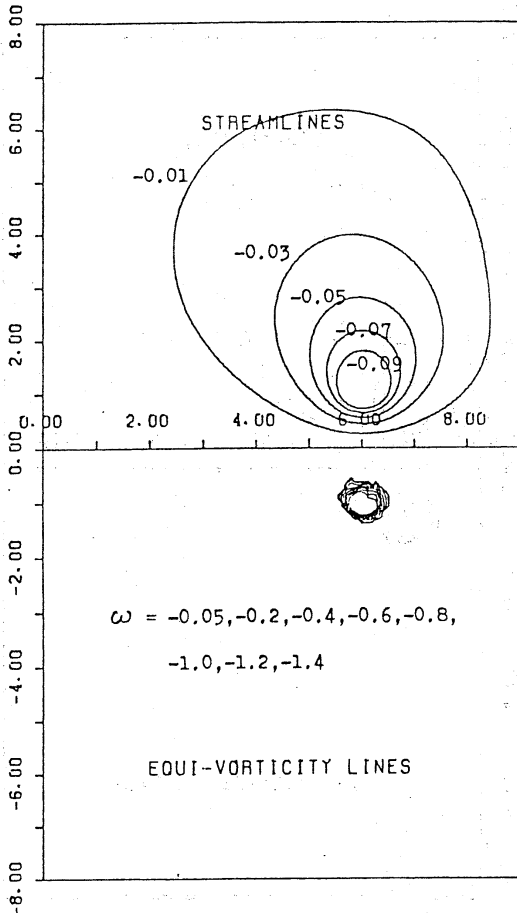
REYNOLDS NUMBER= 500.0

Fig.2(a)

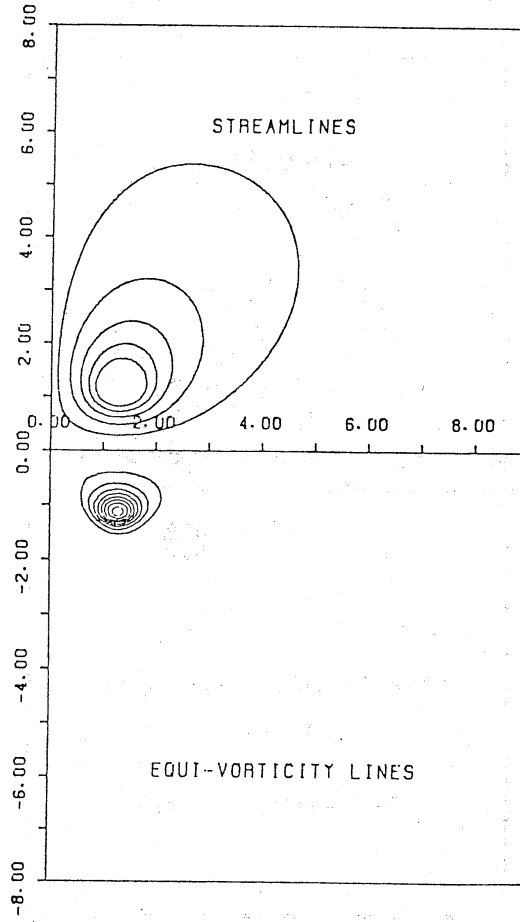




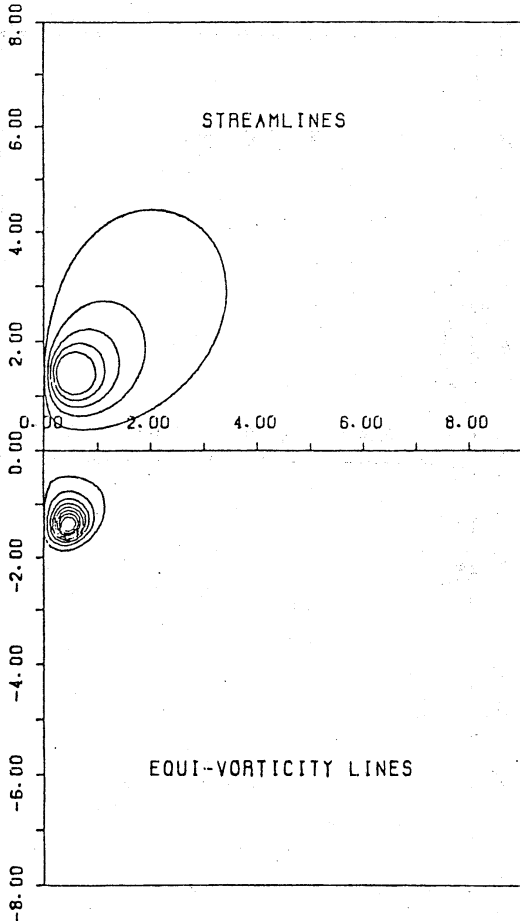
T= 0.00 (6.035, 0.996)



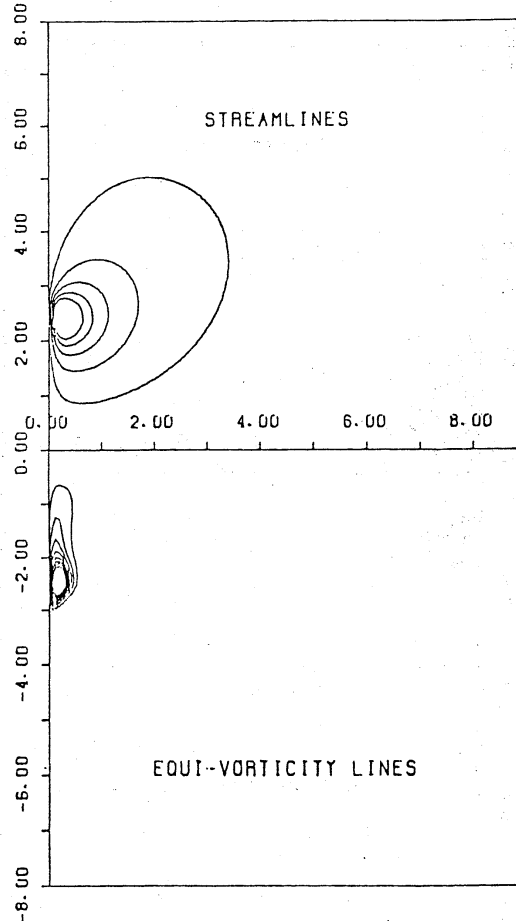
T= 39.80 (1.335, 1.004)



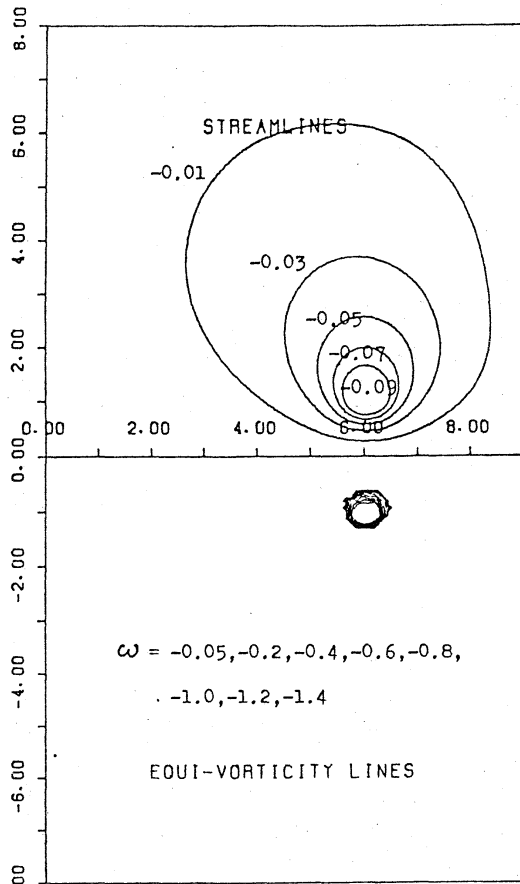
T= 49.80 (0.537, 1.237)



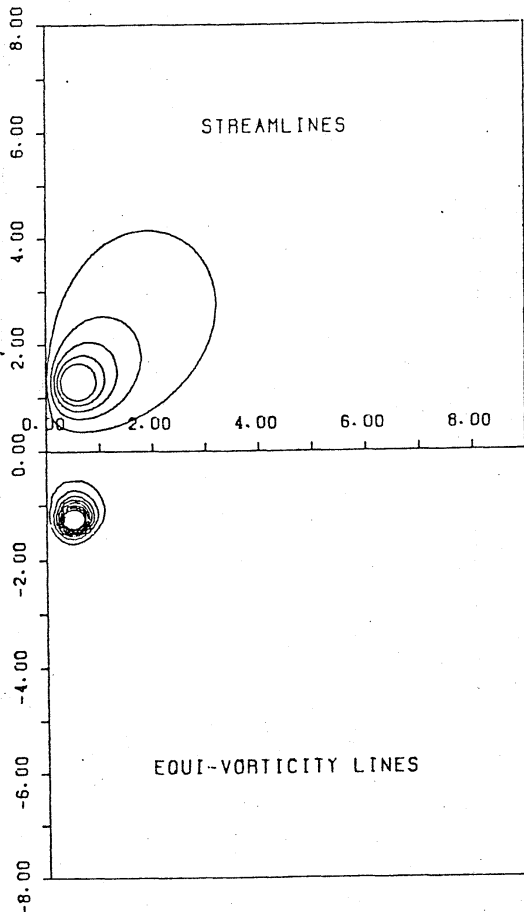
T= 59.80 (0.258, 2.141)



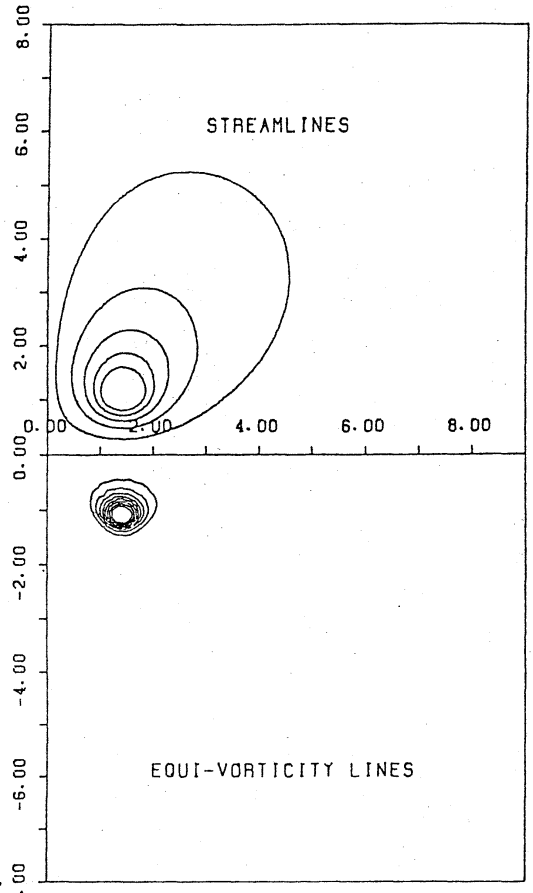
T= 0.00 (6.050, 0.986)



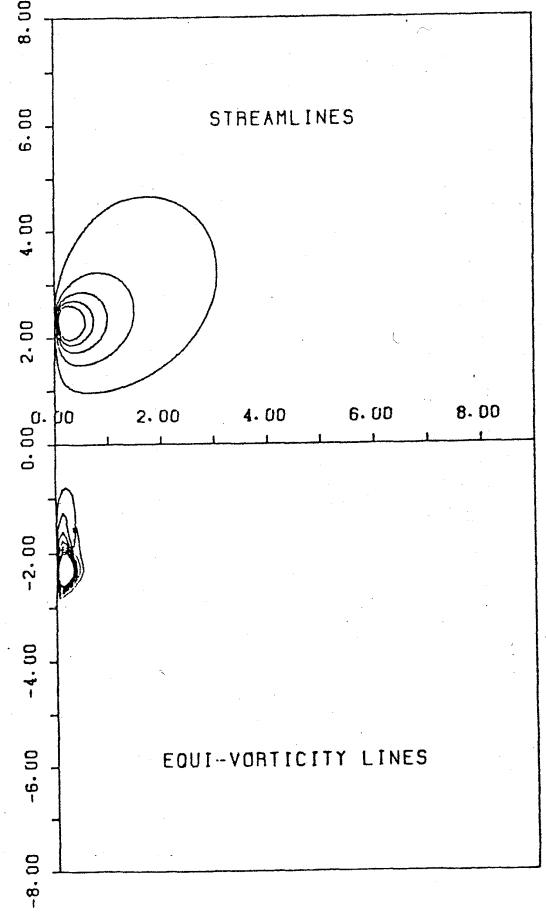
T= 49.80 (0.548, 1.169)



T= 39.80 (1.431, 0.996)



T= 59.80 (0.200, 2.145)



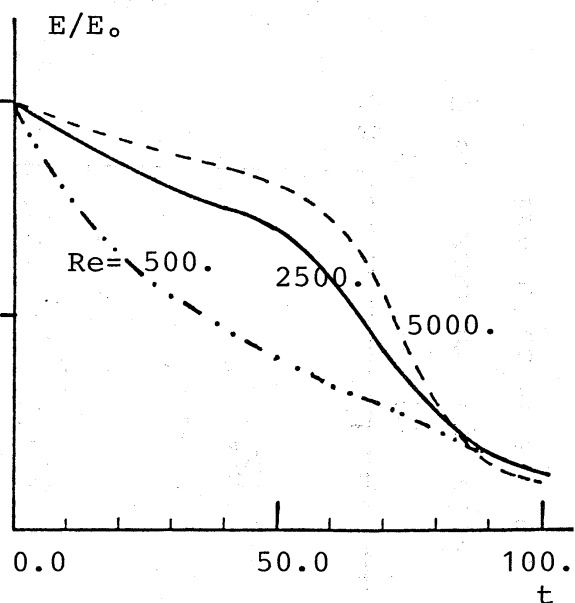
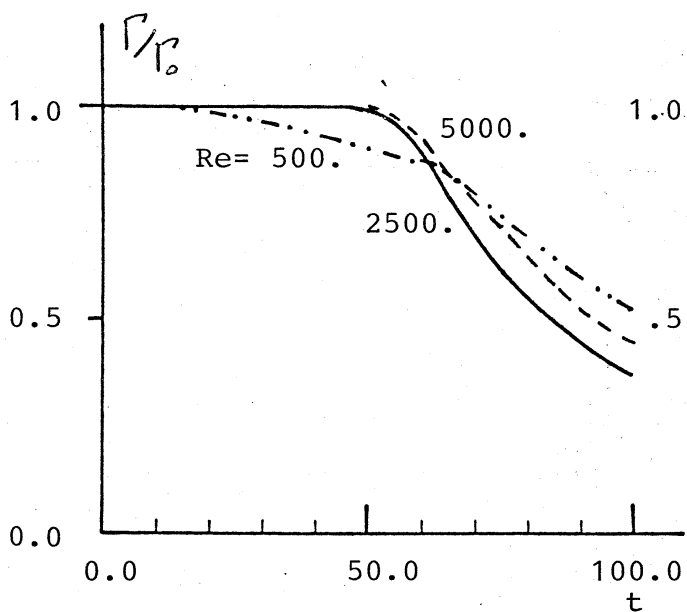
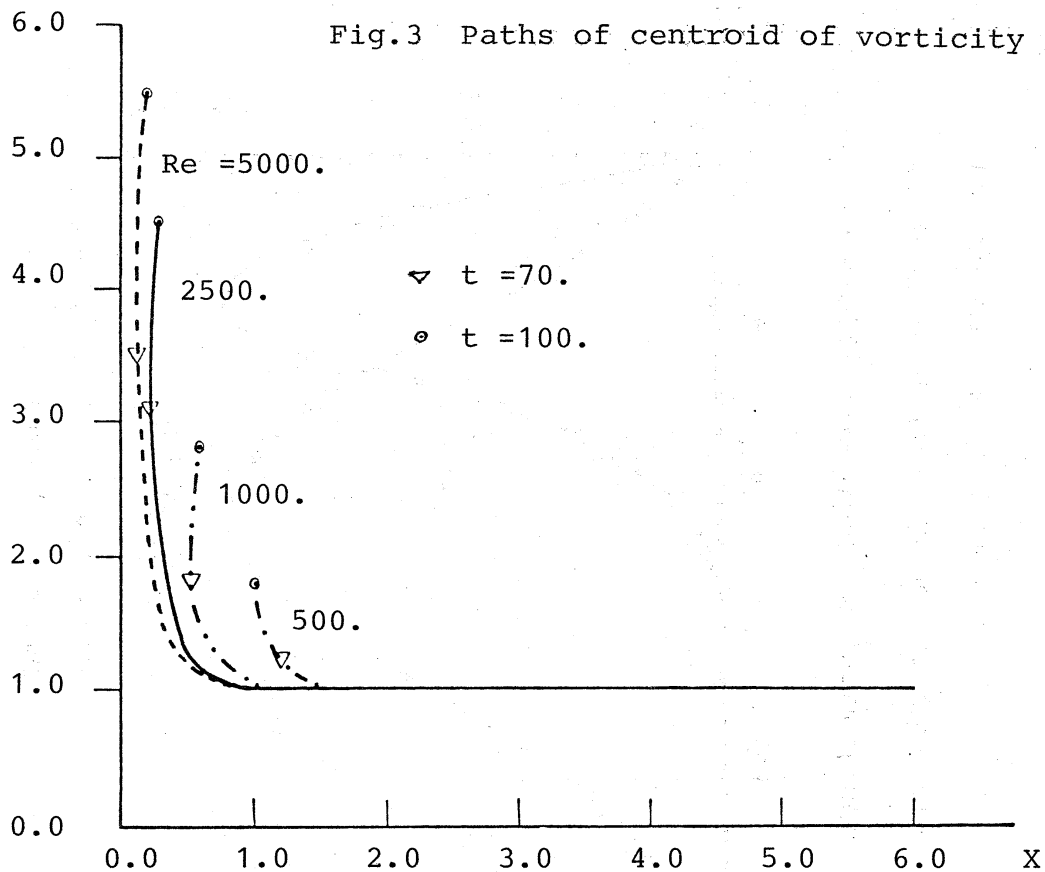


Fig.4 Circulation normalized by the value at t=0.

Fig.5 Total energy normalized by the value at t

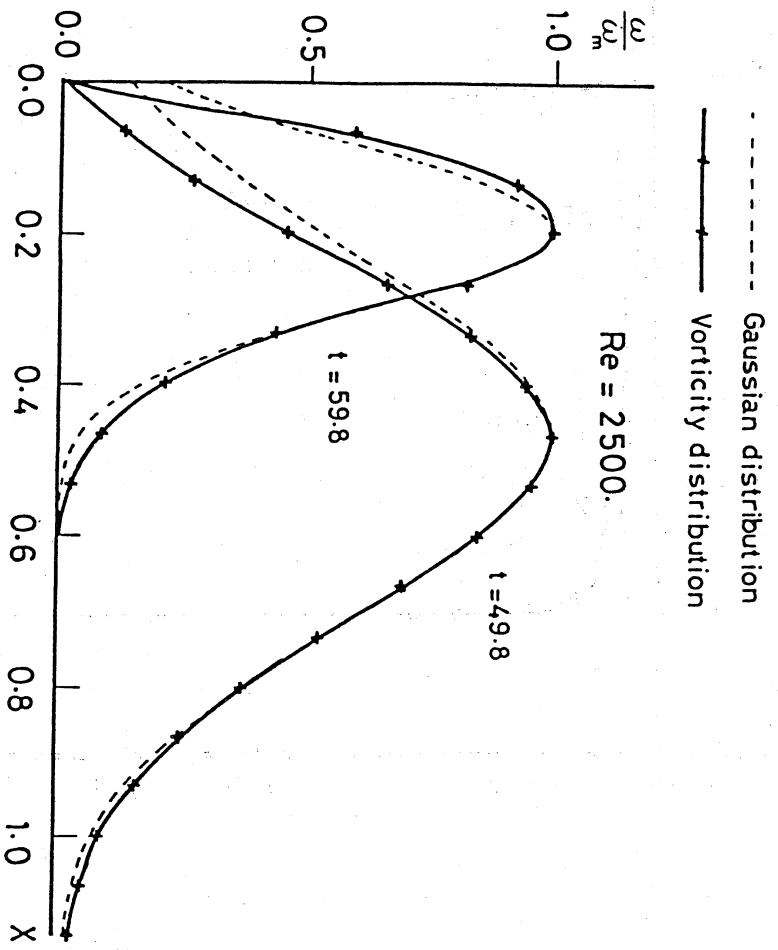


Fig.6 Vorticity distribution (normalized by the maximum value ω_m) along the core axis parallel to the symmetric axis X .

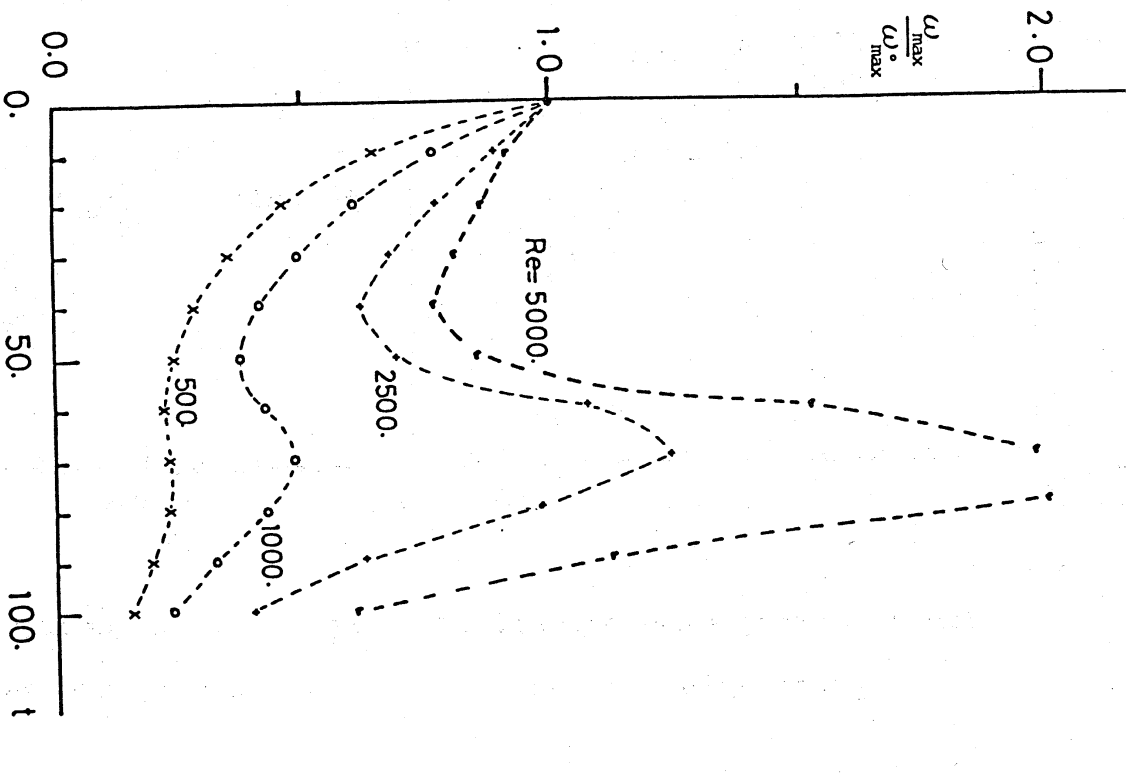


Fig.7 Maximum vorticity, normalized by the value at $t = 0$.